COMPDYN 2015
5th ECCOMAS Thematic Conference on
Computational Methods in Structural Dynamics and Earthquake Engineering
M. Papadrakakis, V. Papadopoulos, V. Plevris (eds.)
Crete Island, Greece, 25–27 May 2015

NUMERICAL ANALYSIS OF THE PLANE WAVES SCATTERING BY SEMI-SPHERICAL ALLUVIAL VALLEY

S L.Chen[1], **X J. Zhu**[2]

[1] Department of Civil Engineering, Nanjing University of Aeronautics and Astronautics
Nanjing, 210016, China
e-mail: iemcsl@nuaa.edu.cn

[2] Department of Civil Engineering, Nanjing University of Aeronautics and Astronautics
Nanjing, 210016, China
zhuxj@nuaa.edu.cn

Keywords: Wave Scattering, Transfer Matrix Method, Transmitting Boundary Condition, Finite Element Method, Semi-Spherical Alluvial Valley.

Abstract. *One of the major concerns of engineering seismology is to understand and explain vibration properties of the soil excited by near earthquakes. Alluvial deposits, often very irregular geometrically, may affect significantly the amplitudes of incident seismic waves. A numerical method is presented for scattering and diffraction of plane waves(SH,P and SV) of arbitrary angle of incidence from three-dimensional complicated topography in this study. The wave input is realized through the free field wave motion obtained by Thomson-Haskell transfer matrix method. The wave motions are calculated by the method of lumped-mass explicit finite element and local transmitting artificial boundary condition. The method is applied to the analytically solved case of semi-spherical alluvial valley on homogenous elastic half space to verify its accuracy.*

1 INTRODUCTION

Topographical and geological irregularities can induce large amplifications and variations in ground motion during earthquakes. The focusing and scattering of the energy carried by seismic waves seem to be the causes of such effects. Large differences of motion between nearby places may be significant in the response of important facilities, like bridges, dams, and life-line systems. Many authors have studied the problem of two-dimensional irregularities for various incident wave fields[3,6-10].Three-dimensional problems have received less attension duo to the increased difficulties which arise in solving this class of problems[1-2,4-5,12-13]. The response of a 3D topography, either a mountain or a canyon, is very sensitive to the azimuth, angle and type of incident wave. To study the half-space problem using the domain discretization technique, such as finite element method and finite difference method, we should introduce a fictitious boundary to make the computation region finite and impose a condition on this boundary to account for the effect of the unbounded medium. The difficulty of wave scattering and diffraction problem solved using numerical method is to deal with the input and the artificial boundary condition. In this paper, a numerical method is presented to solve wave scattering and diffraction problem conveniently.

2 METHOD OF ANALYSIS

The three-dimensional model to be analyzed is shown in Fig.1. It consists of a semi-spherical valley of radius r. The soil is assumed to be elastic, isotropic and homogeneous, and the contact between the valley and the half-space is assumed to be welded. The material properties are given by mass density ρ ,the velocity of the shear waves β and Poisson ratio ν. The subscript R designates these constant in the valley and E in half space. We assume that the half-space is subjected to the incident plane wave traveling upward and to the right along a ray which makes an angle θ with the z axis . The solution of this problem has been obtained by F.J.Sanchez-Sesma(1983,1989).

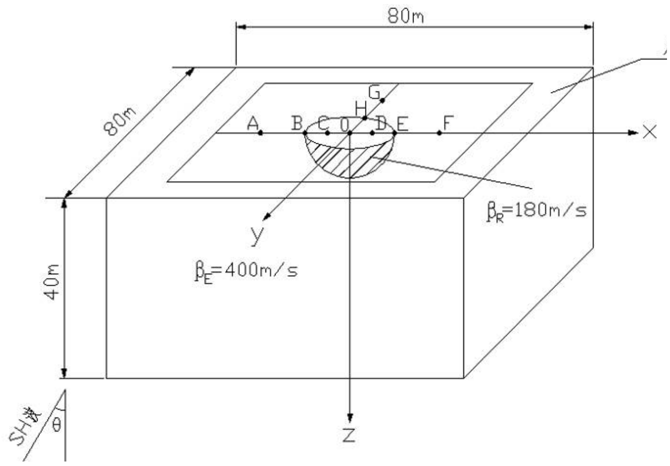

Figure.1 semi-spherical valley and the surrounding half-space

2.1 Input of the Scattering Problem

The incident waves come from the domain exterior to the computation region. Far from the valley the incident waves are reflected from the free surface and incident and reflected waves interfere to give the resulting free-field motion u_f. Close to the valley, the total motion u

comprises of the free-field motion u_f and the waves u_s, reflected and diffracted by the material discontinuity. That is

$$u = u_f + u_s \tag{1}$$

For the interior node, the total displacement can be obtained through finite element method. For the artificial boundary node, the diffraction displacements u_s can be calculated through artificial boundary condition and the total displacements can be obtained by superposition of $(u_s + u_f)$. The free-field motion can be obtained through Thomson-Haskell transfer matrix method[11]. The governing equations of the interior nodes and the boundary nodes may be formulated as follows.

2.2 Governing Equations of the Interior Nodes

The governing equations of the interior nodes may be set up using the standard finite element technique. What should be noted is that the lumped-mass formulation is suggested for the spatial discretization in this study. This is because not only the lumped-mass formulation is much more practical than the consistent-mass for large-scale computations, but also it is the simplest manner to reflect the local feature of wave motion. The governing equations of the interior nodes are written in the following form (Z.P.Liao,2002)

$$m_i \ddot{\boldsymbol{u}}_i + \boldsymbol{F}_i - \boldsymbol{P}_i = 0 \tag{2}$$

where,

$$\left.\begin{array}{l} m_i = \sum\limits_{e} \sum\limits_{j} M_{ij}^{e} \\ M_{ij}^{e} = \int\limits_{V_e} N_i \rho N_j \mathrm{d}V_e \end{array}\right\} \qquad \left.\begin{array}{l} \boldsymbol{F}_i = \sum\limits_{e} \boldsymbol{f}_i^{e} \\ \boldsymbol{f}_i^{e} = \int\limits_{V_e} (\mathbf{L}\mathbf{N}_i)^T \boldsymbol{\tau} dV_e \end{array}\right\} \tag{3}$$

$$\boldsymbol{P}_i = \sum_{e} \left[\int\limits_{V_e} N_i \boldsymbol{g} dV_e + \int\limits_{S_e} N_i \boldsymbol{\tau}_b dS_e \right] \tag{4}$$

$$L = \begin{bmatrix} \partial / \partial_{x_1} & 0 & 0 \\ 0 & \partial / \partial_{x_2} & 0 \\ 0 & 0 & \partial / \partial x_3 \\ \partial / \partial_{x_2} & \partial / \partial_{x_1} & 0 \\ 0 & \partial / \partial_{x_3} & \partial / \partial_{x_3} \\ \partial / \partial_{x_3} & 0 & \partial / \partial_{x_1} \end{bmatrix} \tag{5}$$

m_i is the lumped mass on node i. $\boldsymbol{N}_i$ is shape function matrix for node i. $\boldsymbol{F}_i$ is the constitutive force vector exerted on node i. $\boldsymbol{P}_i$ is a given external force vector exerted on node i, $\boldsymbol{g}$ is the body force,

$\boldsymbol{\tau}_b$ is the stress vector prescribed on boundary.

Assuming the linear viscoelastic constitutive relationship and using central difference integral scheme, Eqn.(2) can be re-written as

$$\boldsymbol{u}_i^{p+1} = 2\boldsymbol{u}_i^p - \boldsymbol{u}_i^{p-1} - \frac{\Delta t^2}{m_i}\left[\sum_e \sum_k K_{l(i)k}^e \boldsymbol{u}_{j(k)}^p + \sum_e \sum_j C_{l(i)k}^e (\boldsymbol{u}_{j(k)}^p - \boldsymbol{u}_{j(k)}^{p-1}) + \boldsymbol{P}_i^p\right] \tag{6}$$

where, $u_i^p = u(p\Delta t, i\Delta x)$, Δt is time step and Δx is spatial step. $K_{l(i)k}^e$ and $C_{l(i)k}^e$ are the element stiffness matrix and element damping matrix, respectively. The subscript $l(i)$ means that the global node index i corresponds to the element local node index l .The subscript $j(k)$ in $\boldsymbol{u}_{j(k)}^p$ means that the global node index j corresponds to the element local node index k . The $\sum_e$ means summation of all elements which includes the global node index i .

2.3 Governing Equations of the Boundary Nodes

The local ABC called as Muti-Transmitting Formula (MTF) is adopted here, which is written as (Z.P.Liao,1996)

$$\bar{u}_{s,0}^{p+1} = \sum_{j=1}^{N} (-1)^{j+1} C_j^N \bar{u}_{s,j}^{p+1-j} \tag{7}$$

where， C_j^N are binomial coefficients.

$$C_j^N = \frac{N!}{(N-j)!\ j!} \tag{8}$$

$$\bar{u}_{s,j}^p = u_s\left(p\Delta t, -jc_a\Delta t\right) \tag{9}$$

N is the approximation order of MTF, c_a is artificial speed. The coordinates $x = -jc_a\Delta t$ indicate the sampling points on the x-axis, which is perpendicular to the artificial boundary at a boundary point under consideration. Since the point $x = -jc_a\Delta t$ do not generally coincide with the discrete nodes $x = -n\Delta x$, in order to implement Eqn.(7), an interpolation scheme is required to express $u_s(t, -jc_a\Delta t)$ in terms of $u_s(t, -n\Delta x)$. After a quadratic interpolation, the second-order ($N = 2$) MTF can be expressed as

$$u_{s,0}^{p+1} = 2\bar{u}_{s,1}^p - \bar{u}_{s,2}^{p-1} = 2\times\sum_{k=1}^{3} t_{1,k} u_{s,k-1}^p - \sum_{k=1}^{5} t_{2,k} u_{s,k-1}^{p-1} \tag{10}$$

$$t_{1,1} = (2-S)(1-S)/2, t_{1,2} = S(2-S), t_{1,3} = S(S-1)/2 \tag{11}$$

$$\left.\begin{array}{l} t_{2,1} = t_{1,1}^2, t_{2,2} = 2t_{1,1}t_{1,2}, t_{2,3} = 2t_{1,1}t_{1,3} + t_{1,2}^2 \\ t_{2,4} = 2t_{1,2}t_{1,3}, t_{2,5} = t_{1,3}^2 \end{array}\right\} \tag{12}$$

where, $S = c_a \Delta t / \Delta x$, $u_{s,j}^p = u_s(p\Delta t, -j\Delta x)$.

Assuming that the responses of the system are known before time $(p+1)\Delta t$, the responses at time $(p+1)\Delta t$ can be calculated as follows

(1) Calculate the free-field displacements using the transfer matrix method[11], and the diffraction displacements at time $p\Delta t$ and $(p-1)\Delta t$ can be obtained through Eqn.(1).

(2) The displacements of interior node at time $(p+1)\Delta t$ can be calculated using Eqn.(6)

(3) Calculate the diffraction displacements of artificial boundary points at time $(p+1)\Delta t$ using Eqn.(10), and the total displacements of artificial boundary points can be obtained by Eqn.(1).

(4) Repeating the steps above, the response of the system can be obtained at successive time.

3 NUMERICAL EXAMPLES

The dimension of the calculation region is $80 \times 80 \times 40m^3$ and $r = 10m$, as shown in Fig.1. The material properties of the valley are: shear wave velocity $\beta_R = 180m/s$,mass density $\rho_R = 3000kg/m^3$,modulus of elasticity $E_R = 1.248 \times 10^9 Pa$,Poisson ratio $v_R = 0.3$ and damping ratio $\xi_R = 0.02$. The material properties of the half space are: $\beta_E = 400m/s$, $\rho_E = 3000kg/m^3$, $E_E = 1.248 \times 10^9 Pa$, $v_E = 0.25$, $\xi_E = 0.02$. Eight-node hexahedron elements are employed and the dimension of the element is about $1m \times 1m \times 1m$. The time step is 0.0005s, and the total time steps is 8192.

The incident wave is shown in Fig.2, which is impulse displacement, and the corresponding spectrum is shown in Fig.3. The incident angle θ is selected as 0^o , 30^o , 60^o and 90^o , respectively.

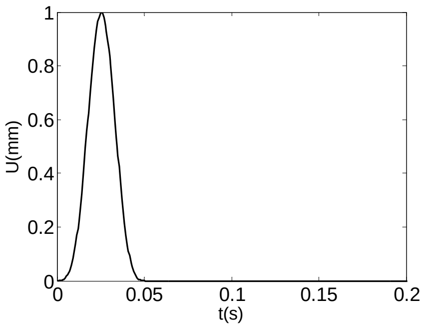

Figure 2. Incident wave

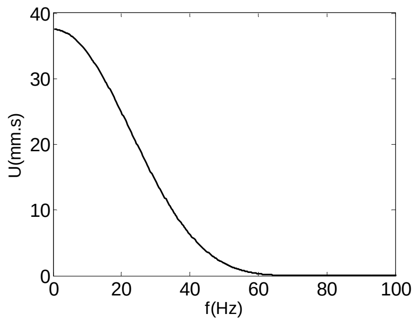

Figure 3. The spectrum of incident wave

3.1 SH wave case

For SH incident wave, this problem was studied by F.J.Sanchez-Sesma(1983,1989). The results are demonstrated as spectral amplification $\left| \frac{U(\omega)}{U_I(\omega)} \right|$ versus dimensionless frequency $\eta = \frac{\omega r}{\pi \beta_E} = \frac{2\pi f r}{\pi \beta_E} = \frac{2r}{\lambda}$, λ is the wavelength. For incident angle 30^o , the displacement spectral amplification along x and y axis, are given in Fig.4-Fig.7.

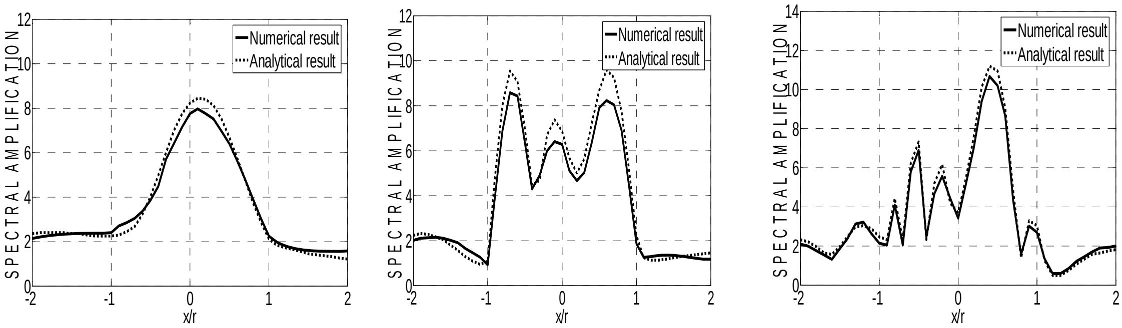

（a） $\eta = 0.5$ （b） $\eta = 1.0$ (c) $\eta = 2.0$

Figure 4 surface spectral amplification of horizontal y-component displacement

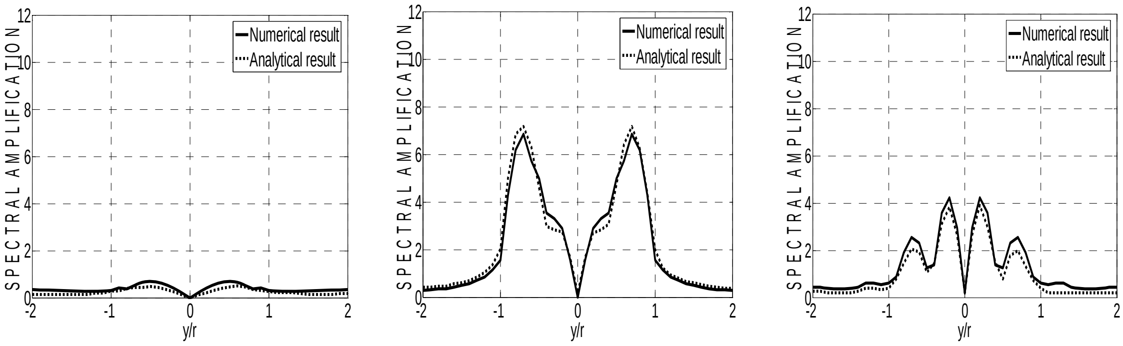

（a） $\eta = 0.5$ （b） $\eta = 1.0$ (c) $\eta = 2.0$

Figure 5 surface spectral amplification of horizontal x-component displacement

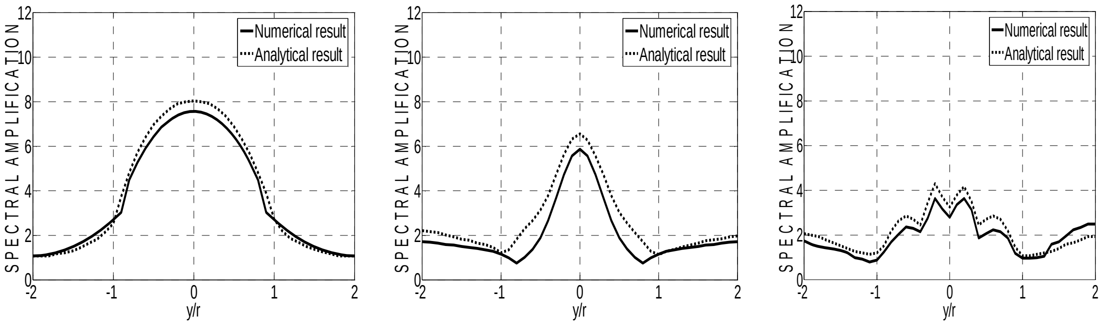

（a） $\eta = 0.5$ （b） $\eta = 1.0$ (c) $\eta = 2.0$

Figure 6 surface spectral amplification of horizontal y-component displacement

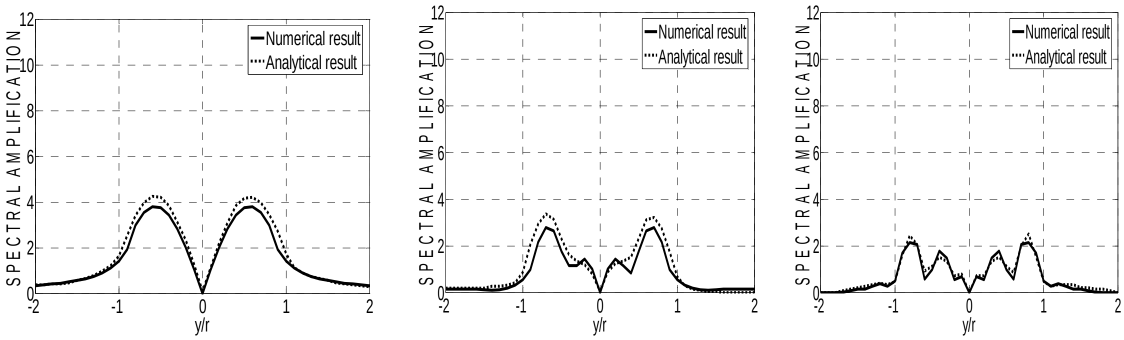

（a） $\eta = 0.5$ （b） $\eta = 1.0$ (c) $\eta = 2.0$

Figure 7 surface spectral amplification of vertical z-component displacement

Fig.4-Fig.7 compares the amplifications obtained by the presented method along the valley with those obtained by J.Sanchez-Sesma(1983,1989), the solid line denotes the numerical results from the proposed method in this study, and the dash line represents the analytical results obtained by J.Sanchez-Sesma(1983,1989). The agreement is very good for both horizontal and vertical component, which tests the accuracy and efficiency of the proposed method.

3.2 P wave case

For comparison with the solution obtained by F.J.Sanchez-Sesma(1983,1989) for incident angle 0^{o}, the displacement spectral amplification are given in Fig.8-Fig.9. The agreement is also very good for both horizontal and vertical component, which further tests the accuracy and efficiency of the proposed method.

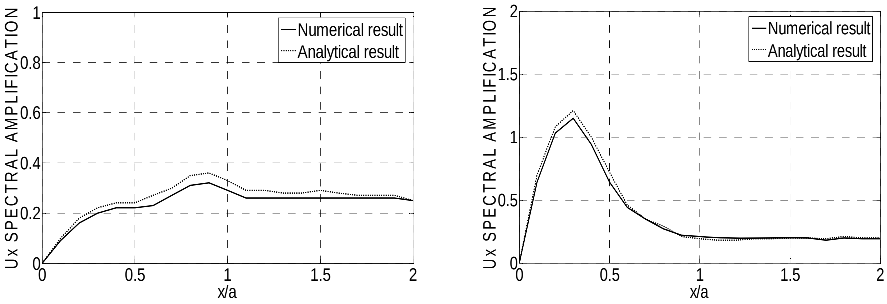

（a） $\eta = 0.5$ （b） $\eta = 1.0$

Figure 8 surface spectral amplification of horizontal x-component displacement

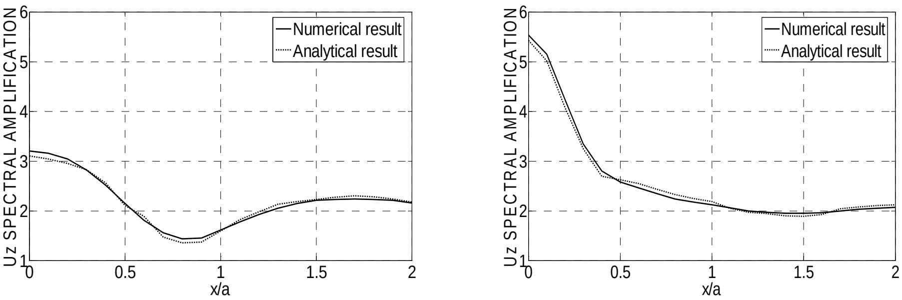

（a） $\eta = 0.5$ （b） $\eta = 1.0$

Figure 9 surface spectral amplification of vertical z-component displacement

4 CONCLUSIONS

A numerical method has been applied to solve the scattering and diffraction of elastic waves by three-dimensional surface irregularities. The method consists of lumped-mass explicit FEM, Multi-transmitting boundary condition and Thomson-Haskell transfer matrix method. The scattering and diffraction of Plane SH and P waves by a semi-spherical valley are analyzed, and the accuracy of this method is validated through comparison with the results of F.J.Sanchez-Sesma(1983,1989). For the fixed geometrical and physical properties of the valley and its surrounding medium, the degree of complexity of the spectral amplification pattern increase with the increase of frequency of the incident waves. The method in this study can be used to arbitrarily irregular topography.

ACKNOWLEDGEMENT

The authors gratefully acknowledge the financial support of this work by the National Natural Science Foundation of China (No.50978135, No.51178222)

REFERENCES

[1] Abdollah Sohrabi-Bidar, Mohsen Kamalian, Effects of three-dimensionality on seismic response of Gaussian-shaped hills for simple incident pulses, *Soil Dynamics and Earthquake Engineering.* **52**,1-12,2013.

[2] E.Reinoso, L.C.Wrobel, Three-dimensional scattering of seismic waves from topographical structures. *Soil Dynamics and Earthquake Engineering.*,**16**,41-61, 1997.

[3] F.J.Sanchez-Sesma, E.Rosenblueth, Ground motion at canyons of arbitrary shape under incident SH waves, *Int.J.Earthquake Eng.Struct.Dyn.*.**7,**441-450,1979.

[4] F.J.Sanchez-Sesma, Diffraction of elastic waves by three-dimensional surface irregularities. *Bull.Seism.Soc.Am.***73,**1621-1636,1983.

[5] F.J.Sanchez-Sesma, Diffraction of elastic waves by three-dimensional surface irregularities Part II. *Bull.Seism.Soc.Am.***79,**101-112,1989.

[6] H.L.Wong, M.D.Trifunac, Scattering of plane SH waves by a semi-elliptical canyon. *Earthquake engineering and structural dynamics,* **3,**157-169,1974.

[7] H.L.Wong, M.D.Trifunac, Surface motion of a semi-elliptical alluvial valley for incident plane SH-waves. *Bull.Seism.Soc.Am.*, **64,**1389-1408,1974.

[8] H.L.Wong, P.C.Jennigs, Effect of canyon topographies or strong ground motion. *Bull.Seism.Soc.Am.***65,**1239-1257,1975

[9] M.D.Trifunc, Surface motion of a semi-cylindrical alluvial valley for incident plane SH-waves. *Bull.Seism.Soc.Am.* **61,**1755-1770,1971.

[10] M.D.Trifunc, Scattering of plane SH waves by a semi-cylindrical canyon. *Earthquake engineering and structural dynamics,* **1**,267-281,1973.

[11] N.Haskell, The dispersion of surface waves in multilayered media, *Bull.Seism.Soc.Am.***43,**17-34,1953.

[12] V.W.Lee, Three-dimensional diffraction of plane P,SV&SH waves by a hemispherical alluvial valley, *Soil Dynamics and Earthquake Engineering.* **3**,133-144,1984.

[13] V.W.Lee， G.Y.Zhu, A note on three-dimensional scattering and diffraction by a hemispherical canyon:Vertically incident plane P-wave. *Soil Dynamics and Earthquake Engineering.* **61**,197-211,2014.

[14] Z.P.Liao, *Introduction to wave motion theories in engineering, 2nd Edition*. Science Press, Beijin, 2002.

[15] Z.P.Liao, Extrapolation non-reflecting boundary conditions,*Wave motion,***24,**117-138,1996.